The first measurement of the differential cross-sections for the electroweak production of ZZ in association with two jets in the four-leptons final state in 13 TeV proton-proton collision with the ATLAS detector.

A Dissertation

Presented to

The Faculty of the Graduate School of Arts and Sciences
Brandeis University

Department of Physics

Professor Gabriella Sciolla, Advisor

In Partial Fulfillment
of the Requirements for the Degree
Doctor of Philosophy

by
Prajita Bhattarai

May 2023

This dissertation, directed and approved by Prajita Bhattarai's Committee, has been accepted and approved by the Faculty of Brandeis University in partial fulfillment of the requirements for the degree of:

DOCTOR OF PHILOSOPHY

Wendy Cadge, Dean
Graduate School of Arts and Sciences

Dissertation Committee:
Professor Gabriella Sciolla, Department of Physics, Brandeis University
Professor Aram Apyan, Department of Physics, Brandeis University
Dr. Alessandro Tricoli, Brookhaven National Laboratory

ABSTRACT

The first measurement of the differential cross-sections for the electroweak production of ZZ in association with two jets in the four-leptons final state in 13 TeV proton-proton collision with the ATLAS detector.

A dissertation presented to the Faculty of the
Graduate School of Arts and Sciences of Brandeis University
Waltham, Massachusetts

By Prajita Bhattarai

Table of Contents

Acknowledgements iv

Abstract iv

List of Tables vii

List of Figures viii

List of Abbreviations ix

I Introduction 1

II Theory 2

1 The Standard Model 3

1.1 Symmetries 3

1.2 Particles and Fields 5

1.3 Theoretical Formulation of the Standard Model 8

2 Limitations of the Standard Model 19

3 Phenomenology of Proton-Proton Collisions 20

4 Electroweak Diboson Physics 24

III The Large Hadron Collider 28

5 ATLAS Detector 28

6 Particle Reconstruction 28

7 Future Upgrades 28

IV Analysis Overview 29

8 Goals 30

9 Datasets and Monte Carlo Simulation 30

10 Phase Space Definition 30
11 Object and Event Selection 30
12 Definition of Measured Observables 30

V Analysis Strategy 31
13 Background Estimation 31
14 Unfolding 31
15 Uncertainties on the Measurement 31

VI Results 32
16 Differential Cross-sections 32
17 Effective Field Theory ReInterpretation 32

VII Conclusion 33

VIII Outlook 34
18 Run-3 34
19 High Luminosity LHC 34

References 35

Appendices 37

Appendices 37

List of Tables

1 Properties of SM gauge bosons. [1] 6

2 Summary of different interactions of fermions under different gauge theory. The check mark suggests that the fermions interact via associated force. . . . 6

3 Electroweak quantum numbers of the SM half-integer spin fermions (quarks and leptons) arranged in a left-handed $SU(2)$ doublet and right-handed $SU(2)$ singlet. [2] 7

List of Figures

1 The seventeen fundamental particles of the SM include three generations of twelve fermions, four gauge bosons, and the scalar Higgs bosons. [3] 5

2 Parton distribution functions $xf_q(x, Q^2)$ for reference momentum transfer $Q_0^2 = 10\ GeV^2$ (left) and $Q_0^2 = 10^4\ GeV^2$ (right). The dependence of momentum fraction z carried by a parton is extracted in global PDF fits from experimental data [4]. 21

3 Phenomenology of di-Z boson production in association with two jets in proton-proton collider 23

4 Typical diagrams for the QCD $\alpha_S^2\alpha_{EWK}^4$ production of $ZZjj$. 25

5 Feynman diagrams at LO for the EWK α_{EWK}^6 production of $ZZjj$. 26

- BSM: Beyond the Standard Model
- C: Charge conjugation
- P: Parity
- T: Time-reversal
- EWK: Electroweak
- H: Weak Hypercharge
- I: Weak Isospin
- $\mathcal{L}_{\mathcal{SM}}$: Lagrangian
- LH: Left Handed
- MC: Monte Carlo
- Q: Electric Charge
- QGC: Quartic Gauge Coupling
- QED: Quantum Electrodynamics
- QCD: Quantum Chromodynamics
- ($\mathcal{P}$): Poincare group
- RH: RightHanded
- SM: Standard Model
- TGC: Triple Gauge Coupling
- VBS: Vector Boson Scattering
- VEV: Vacuum Expectation Value

Chapter I: Introduction

Chapter II: Theory

This chapter describes the theoretical framework of the experimental measurements discussed in this thesis. The Standard Model (SM) of particle physics is introduced, and concepts relevant to the thesis are discussed in Section 1. Section 2 discusses the outstanding problems with the Standard Model, thus, motivating the experimental measurement. Section 3 discusses the phenomenology of the proton-proton collisions relevant to this thesis whereas, Section 4 discusses the physics of two Z bosons production in association of two jets.

1 The Standard Model

The SM of particle physics is a mathematical framework based on quantum field theory which incorporates quantum mechanics and special relativity. The SM describes all known fundamental particles in nature and their interactions. It consists of two sets of particles with intrinsic angular momentum, half-integer-spin fermions that are fundamental constituents of matter particles, and force-carrying integer-spin bosons. The seventeen fundamental particles of the SM and their properties such as mass, charge, and intrinsic spin are shown schematically by figure 1. Discussion in this section is written with the guidance from two textbooks on particle physics, Mark Thomson's Modern Particle Physics [5], and Halzen & Martin's Quarks & Leptons [2].

1.1 Symmetries

The fundamental particles of the SM and their interactions can be described by constructing a general renormalizable Lagrangian ($\mathcal{L}_{SM}$) that respects certain sets of given symmetries. The Lagrangian of the SM is independent of the reference frame, naturally respecting the complete external symmetries of special relativity, the Poincare group ($\mathcal{P}$). Thus, the SM is invariant under spacetime translations, boosts, and rotations. Additionally, by the construction of the Lagrangian, the SM respects an internal local gauge symmetry $SU(3)_C \otimes SU(2)_L \otimes U(1)_Y$. The $SU(3)_C$ symmetry is associated with the Quantum Chromodynamics (QCD) discussed in detail in Section 1.3.4. The $SU(2)_L \otimes U(1)_Y$ gauge symmetry discussed in 1.3.5 is associated with the unified electroweak theory that combines Quantum Electrodynamics (QED) and the weak interactions.

According to Noether's theorem, a quantity is conserved for each continuous transformation that leaves the Lagrangian invariant [6]. Several interesting physical quantum numbers are conserved as a consequence of the symmetries respected by the SM. The $SU(3)_C$ in QCD conserves color charge. Weak isospin (I) and weak hypercharge (Y) are the quantum

numbers associated with the $SU(2)_L$ and $U(1)_Y$ gauge groups respectively. At low energies the $SU(2)_L \otimes U(1)_Y$ symmetry is spontaneously broken and will be discussed in Section 1.3.5. The $SU(2)_L$ group follows a chiral structure where the gauge fields couple explicitly to the left-handed (LH) chiral fermions states and the right-handed (RH) chiral anti-fermions states.

The SM also respects CPT symmetry, a combination of three additional discrete symmetries, charge conjugation (C), parity (P), and time-reversal (T). The charge-conjugation transformation transforms particles to anti-particles by reversing the quantum numbers, whereas, the parity transformation transforms left-handed particles to right-handed particles.

1.2 Particles and Fields

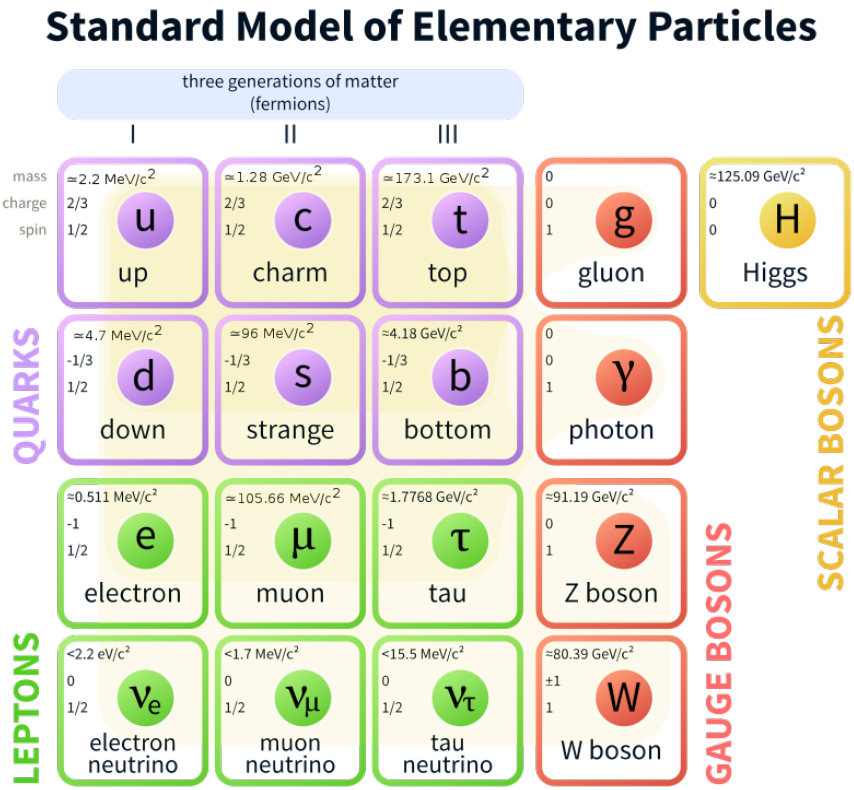

Figure 1: The seventeen fundamental particles of the SM include three generations of twelve fermions, four gauge bosons, and the scalar Higgs bosons. [3]

The twelve half-integer-spin fermions can be distinguished further into two categories, leptons, and quarks, each having three generations of particles with similar properties as shown schematically by figure 1. For each fermion, there exists an anti-fermion with the same additive quantum numbers but with opposite signs. Four spin 1 bosons shown in Table 1 are collectively called the gauge bosons. Quanta of these gauge fields mediate the electromagnetic, weak, and strong interactions and are invariant under various local gauge transformations [7]. As summarized by Table 2, fermions take part in different interactions. The strength of interaction is governed by a gauge coupling parameter.

Massless photon (γ) mediates the electromagnetic interaction. The massive W and Z

Table 1: Properties of SM gauge bosons. [1]

Interaction Type		Particle	Q	Mass $[GeV]$	Symmetry Group
Electroweak	Electromagnetic	Photon (γ)	0	0	$SU(2) \otimes U(1)$
	Weak	$W^{\pm}$	± 1	80.4	
		Z boson	0	91.2	
Strong		gluons (g)	0	0	$SU(3)$

Table 2: Summary of different interactions of fermions under different gauge theory. The check mark suggests that the fermions interact via associated force.

Particles		Strong $SU(3)$	Electromagnetic $U(1)$	Weak $SU(2)$
Quarks	u, c, t d, s, b	✓	✓	✓
Leptons	e, μ, τ	-	✓	✓
	ν_e, ν_μ, ν_τ	-	✓	-

bosons mediate weak interaction. The electric charge (Q) which is conserved in all interactions is related to the isospin and hypercharge by $Q = I_3 + \frac{Y}{2}$, where I_3 is the third component of the weak isospin. As a consequence of the chiral structure of $SU(2)_L$, each generation of fermion contains a left-handed doublet with $I_3 = \pm\frac{1}{2}$ and a right-handed singlet carrying $I_3 = 0$ which are shown in Table 3.

Each generation of lepton, electron (e), muon (μ) and tau (τ) is accompanied by a neutral particle called neutrino (ν) with same lepton flavor ($\nu_e, \nu_\mu \& \nu_\tau$). The SM neutrinos are their own anti-particles and only left-handed neutrinos are predicted by the theory. The lepton flavor is conserved by the SM in all interactions.

The quarks can be further categorized into two categories, the up-type quarks with $+\frac{2}{3}$ charge and the down-type quarks with $-\frac{1}{3}$ charge. Up (u), charm (c) , & top (t) are the first, second, and third generation of the up-type quarks, while the down (d), strange (s) & bottom (b) are the three generations of the down-type quarks. The down-type left-handed quarks in $SU(2)_L$ quark doublets d', s' & b' summarized in table 3 are linear combinations of d, s, b quarks. The quarks interact strongly with one another by strong interaction mediated by

Table 3: Electroweak quantum numbers of the SM half-integer spin fermions (quarks and leptons) arranged in a left-handed $SU(2)$ doublet and right-handed $SU(2)$ singlet. [2]

Particle Types	First	Second	Third	I_3	Y	Q
Leptons	$\begin{pmatrix} e \\ \nu_e \end{pmatrix}_L$	$\begin{pmatrix} \mu \\ \nu_\mu \end{pmatrix}_L$	$\begin{pmatrix} \tau \\ \nu_\tau \end{pmatrix}_L$	$-\frac{1}{2}$ $\frac{1}{2}$	-1 -1	-1 0
	e_R	μ_R	τ_R	0	-2	-1
Quarks	$\begin{pmatrix} u \\ d' \end{pmatrix}_L$	$\begin{pmatrix} c \\ s' \end{pmatrix}_L$	$\begin{pmatrix} t \\ b' \end{pmatrix}_L$	$\frac{1}{2}$ $-\frac{1}{2}$	$\frac{1}{3}$ $\frac{1}{3}$	$\frac{2}{3}$ $-\frac{1}{3}$
	u_R	c_R	t_R	0	$\frac{4}{3}$	$\frac{2}{3}$
	d_R	s_R	b_R	0	$-\frac{2}{3}$	$-\frac{1}{3}$

the massless neutral gluons which follow from $SU(3)$ gauge symmetry by exchange of color charges. Each quark can have either one of the three color charges (red, blue &, green), whereas an anti-quark can have either an anti-red, anti-blue or anti-green color charge. There are eight gluons in the SM with color charges formed by a combination of either of the two color charges. Since gluons have a color charge, they interact with other gluons strongly. Only color neutral hadronic states formed by a combination of quarks and gluons are observed experimentally.

Higgs boson is the only spin-0 scalar particle in the theory with no charge and gives masses to all other particles through Spontaneous Symmetry Breaking which will be discussed in Section 1.3.5.

1.3 Theoretical Formulation of the Standard Model

1.3.1 Relativistic Quantum Field Theory

Relativistic quantum field theory is the theoretical framework of the SM that describes elementary particles and their interactions. This section introduces the framework.

1.3.2 Lagrangian of the Standard Model

The dynamics of the SM can be described by the Lagrangian density given in equation 1.1 which is invariant under the local gauge transformation of the $SU(3) \otimes SU(2)_L \otimes U(1)_Y$ symmetry group.

$$\mathcal{L}_{\mathcal{SM}} = -\frac{1}{4}F_{\mu\nu}F^{\mu\nu} + i\bar{\psi}\gamma^{\mu}D_{\mu}\psi + |D_{\mu}\phi|^2 + -V(\phi) + \bar{\psi}_i y_{ij}\psi_j\phi + h.c. \tag{1.1}$$

The first term $-\frac{1}{4}F_{\mu\nu}F^{\mu\nu}$ describes the dynamics of the gauge boson interactions, the second term $i\bar{\psi}\gamma^{\mu}D_{\mu}\psi$ describes the interaction of the fermion fields. The third term $|D_{\mu}\phi|^2$ describes the couplings between the Higgs boson and gauge bosons, whereas the term $V(\phi)$ describes the Higgs potential and its self-interactions. The second last term $\bar{\psi}_i y_{ij}\psi_j\phi$ generates masses for fermions based on their Yukawa couplings y_{ij} to the Higgs field. Similarly, the last term $h.c.$ generates masses for antifermions.

1.3.3 Quantum Electrodynamics

Quantum electrodynamics describes electromagnetic interaction. The Lagrangian density ($\mathcal{L}_{Dirac}$) describes the free propagation of a fermion in a vacuum as:

$$\mathcal{L}_{Dirac} = \bar{\psi}i\gamma^{\mu}\partial_{\mu}\psi - m\bar{\psi}\psi \tag{1.2}$$

,

where ψ is the fermionic spinor, γ^μ represents the Dirac matrices with μ being the Lorentz index running from 0 to 3, ∂^μ is the covariant derivative and m is the mass of the fermion.

The Lagrangian in equation 1.2 is invariant under a $U(1)$ global gauge transformation,

$$\psi \rightarrow \psi^{'} = e^{iq\alpha}\psi, \tag{1.3}$$

where q is a parameter of the transformation itself and α is a real phase factor. However, under the local gauge transformation of form

$$\psi \rightarrow \psi^{'} = e^{iq\alpha(x)}\psi \tag{1.4}$$

which α depends on $x = (x_0, x_1, x_2, t)$ the Dirac Lagrangian in equation 1.2 is not invariant.

To make the Lagrangian of equation 1.2 invariant, a gauge field A_μ is introduces with the following transformation properties,

$$A_\mu \rightarrow A_\mu - \partial_\mu \alpha \tag{1.5}$$

The A_μ couples to fermionic fields $\psi(x,t)$ with strength q. A covariant derivative specific to the local gauge transformation is defined as:

$$D_\mu = \partial_\mu - iqA_\mu \tag{1.6}$$

The quantity q can be interpreted as the electric charge $-e$ of fermion which gives the coupling strength of QED. With these substitutions, the Dirac Lagrangian in equation 1.2 changes to following

$$\mathcal{L} = \bar{\psi}(i\gamma^\mu D_\mu - m)\psi \tag{1.7}$$

,

which is invariant under $U(1)$ gauge transformation respecting the $U(1)$ gauge symmetry.

The gauge field A_μ can be interpreted as the photon field and is related to the electromagnetic field tensor by

$$F_{\mu\nu} = \partial_\mu A_\nu - \partial_\nu A_\mu \tag{1.8}$$

The gauge invariant kinetic term of photon $-\frac{1}{4}F_{\mu\nu}F^{\mu\nu}$ can be inserted into the Lagrangian in equation 1.7 which gives us the full Lagrangian of QED invariant under $U(1)$ gauge transformation.

$$\mathcal{L}_{QED} = -\frac{1}{4}F_{\mu\nu}F^{\mu\nu} + \bar{\psi}(i\gamma^\mu D_\mu \ - \ m)\psi \tag{1.9}$$

$\mathcal{L}_{QED}$ in equation 1.9 is the full Lagrangian for QED and the electromagnetic phenomena can be derived by solving for the equations of motion applying the Lorentz gauge condition $\partial_\mu A^\mu = 0$.

1.3.4 Quantum Chromodynamics

Interaction between the quarks is defined by Quantum Chromodynamics requiring $SU(3)$ gauge transformation on the quark field with color charge j (red, blue, or green).

The Dirac Lagrangian for a quark can be modified to include all possible colors of quark field q_j as

$$\mathcal{L} = \bar{q_j}(i\gamma^\mu\partial_\mu - m)q_j \tag{1.10}$$

The generators of the $SU(3)$ group are eight linearly independent traceless Gell-Mann matrices that do not commute with each other such that

$$[T_a, T_b] = if_{abc}T_c \tag{1.11}$$

where f_{abc} is the structure constant of $SU(3)$

The local $SU(3)$ gauge transformation is

$$q(x) \rightarrow e^{i\alpha_a(x)T_a} q(x) \tag{1.12}$$

where $T_a = \frac{\lambda_a}{2}$, and $a = 1, 2...8$. To understand the source of gauge invariance in the Lagrangian in equation , we can consider an infinitesimal transformation of the color field as

$$q(x) \rightarrow [1 + i\alpha_a(x)T_a]q(x) \ni \ \partial_\mu q \rightarrow (1 + i\alpha_a T_a)\partial_\mu q + iT_a q\partial_\mu \alpha_a \tag{1.13}$$

The last term $iT_a q\partial_\mu \alpha_a$ breaks the gauge invariance. Similar to QED, eight gauge fields corresponding to each $a = 1, 2...8$ G^a_μ with following transformation properties are introduced

$$G^a_\mu \rightarrow G^a_\mu - \frac{1}{g_s}\partial_\mu \alpha_a - f_{abc}\alpha_b G^c_\mu \tag{1.14}$$

These gauge fields G^a_μ are the gluon fields. Similar to QED the covariant derivative is defined as

$$D_\mu = \partial_\mu + ig_s \frac{\lambda_a}{2} G^a_\mu \tag{1.15}$$

where g_s is the coupling strength of the gluon fields to the quark fields.

The Lagrangian density in equation 1.10 is then

$$\mathcal{L} = \bar{q_j}(i\gamma^\mu D_\mu - m)q_j \tag{1.16}$$

Similar to QED, a gauge-invariant kinetic term $-\frac{1}{4}G^a_{\mu\nu}G^{\mu\nu}_a$,

dependent on the field strength tensor $G^a_{\mu\nu}$ is added to equation 1.16 to give the full QCD Lagrangian. The kinetic terms allow self-interaction within the gluon fields which is an important feature of QCD. $G^a_{\mu\nu}$ is the field strength tensor defined as

$$G^a_{\mu\nu} = \partial_\mu G^a_\nu - \partial_\nu G^a_\mu - g_s f_{abc} G^b_\mu G^c_\nu \tag{1.17}$$

Therefore, the complete $SU(3)$ gauge invariant Lagrangian describing the quarks and gluons interaction is

$$\mathcal{L}_{QCD} = \bar{q_j}(i\gamma^\mu D_\mu - m)q_j - \frac{1}{4}G^a_{\mu\nu}G^{\mu\nu}_a \tag{1.18}$$

1.3.5 Electroweak Theory

Weak interactions describe the interactions mediated by massive gauge bosons. The first formulation of the weak interaction was made by Fermi in 1934, to explain the beta decay using four fermion interaction vertex. The formulation successfully describes the beta decay at low energies when the interaction energy is much smaller than the W boson mass. A unified electroweak theory was formulated by Glashow in 1961 [8], by extending the $SU(2)$ symmetric non-Abelian gauge theory formulated by Yang and Mills in 1954 [9] to $SU(2) \otimes U(1)$ gauge theory. Above the unification threshold, the differences in the electromagnetic and weak interactions are not apparent.

Experimental observations suggest that weak interactions violate parity by only affecting the left-handed fermion fields and the right-handed anti-fermion fields. Thus the unified electroweak theory are described by $SU(2)_L \otimes U(1)_Y$ gauge interactions. Similar to the electric charge Q conserved in QED by $U(1)$ symmetry, the weak hypercharge ($Y = 2(Q - I_3)$) related to the electric charge and the weak isospin I_3) is conserved by the $U(1)_Y$ symmetry. The fermion fields are represented by the left-handed doublets χ_L and the right-handed singlets ψ_R, introduced in table 3. The doublet and singlet field for the first generation of leptons and quarks are,

$$\chi_L = \begin{pmatrix} \nu_e \\ e \end{pmatrix}_L \quad \& \quad \chi_L = \begin{pmatrix} u \\ d \end{pmatrix}_L$$
$$\psi_R = e_R \quad \& \quad \psi_R = u_R \;\&\; d_R$$

The Lagrangian for these fermion fields should be invariant under local gauge transformation corresponding to both $SU(2)_L$ and $U(1)_Y$ symmetry as,

$$\chi_L \rightarrow e^{i\beta(x)Y + i\alpha_a(x)\tau_a}\chi_L \tag{1.19}$$

$$\psi_R \rightarrow e^{i\beta(x)Y}\psi_R \tag{1.20}$$

where, $\beta(x)$ and $\alpha(x)$ are the local phase transformation for $U(1)_Y$ and $SU(2)_L$ symmetry groups respectively. Weak hypercharge operator Y and Pauli matrices $\tau_{a=1,2,3}$ are generators of $U(1)_Y$ and $SU(2)_L$ symmetry groups respectively. Similar to the formulation in QED and QCD discussed in Section 1.3.3 and 1.3.4, four new field strength tensors $B_{\mu\nu}$ and $W^a_{\mu\nu}$ corresponding to respectively the $U(1)_Y$ and $SU(2)_L$ transformations are introduced. The $SU(2)_L \otimes U(1)_Y$ gauge-invariant Lagrangian for a massless fermion and massless gauge fields is:

$$\mathcal{L}_0 = \bar{\chi_L}\gamma^\mu[i\partial_\mu - g\frac{\tau_a}{2}W^a_\mu + \frac{g^{'}}{2}B_\mu]\chi_L + \bar{\psi_R}\gamma^\mu[i\partial_\mu + g^{'}B_\mu]\psi_R - \frac{1}{4}W^a_{\mu\nu}W^{\mu\nu}_a - \frac{1}{4}B_{\mu\nu}B^{\mu\nu} \tag{1.21}$$

where similar to QED and QCD, the field strength tensors are defined in terms of the covariant derivative to preserve the gauge-invariance in the kinetic terms as,

$$B_{\mu\nu} = \partial_\mu B_\nu - \partial_\nu B_\mu \tag{1.22}$$

$$W^a_{\mu\nu} = \partial_\mu W^a_\nu - \partial_\nu W^a_\mu + g\epsilon^{abc}W^b_\mu W^c_\nu \tag{1.23}$$

The non-Abelian part of the $SU(2)_L$ transformation is represented by the last term of equation 1.23 which gives the quartic and triple self-interactions between the gauge bosons with coupling strength g.

The electroweak Lagrangian in equation 1.21 contains two terms, one of which gives rise to the charged-current interaction with the two $SU(2)$ boson field

$$W_\mu^\pm \;=\; \frac{W_\mu^1 \mp iW_\mu^2}{\sqrt{(2)}} \tag{1.24}$$

via exchange of the $W^\pm$ bosons and the neutral current interactions from the two neutral gauge boson fields W_μ^3 and B_μ.

The Lagrangian for the charged-current interaction for the first generation of quarks and leptons is,

$$\mathcal{L}_{CC} = \frac{g}{2\sqrt{2}}\{W_\mu^\dagger[\bar{u}\gamma^\mu(1-\gamma_5)d + \bar{\nu_e}\gamma^\mu(1-\gamma_5)e] \;+\; h.c\} \tag{1.25}$$

The $SU(2)_L$ charged-current interaction Lagrangian for the next two generations follows the same, establishing the universality of the quark and lepton interactions as a direct consequence of the gauge symmetry.

The neutral-current Lagrangian is given by,

$$\mathcal{L}_{NC} = \sum_j \bar{\psi_j}\gamma^\mu\{A_\mu[g\frac{\tau_3}{2}sin\theta_W + g^{'}Ycos\theta_W] + Z_\mu[\frac{\tau_3}{2}cos\theta_W - g^{'}Ysin\theta_W]\}\psi_j \tag{1.26}$$

where the two neutral gauge fields Z_μ and A_μ associated with Z boson and photon governing the weak neutral and electromagnetic interactions are obtained from an arbitrary linear combination of the W_μ^3 and B_μ fields as

$$\begin{pmatrix} A_\mu \\ Z_\mu \end{pmatrix} = \begin{pmatrix} cos\theta_W & sin\theta_W \\ -sin\theta_W & cos\theta_W \end{pmatrix} \begin{pmatrix} B_\mu \\ W_\mu^3 \end{pmatrix} \tag{1.27}$$

The following condition needs to be imposed to get QED from A_μ:

$$gsin\theta_W = g^{'}cos\theta_W = e \;\&\; Y = Q - T_3 \tag{1.28}$$

, where $T_3 = \frac{\tau_3}{2}$ is the weak isospin and θ_W is the Weinberg mixing angle, which can be measured experimentally and expressed in terms of the two $SU(2)_L$ coupling $g^{'}$ and $U(1)_Y$

coupling g as:

$$sin\theta_W = \frac{g^{'}}{\sqrt{g^2 + g^{'2}}} \;\&\; cos\theta_W = \frac{g}{\sqrt{g^2 + g^{'2}}} \tag{1.29}$$

The Lagrangian in equation 1.21 describes the electroweak interactions only for massless fermions and massless gauge bosons, which contradicts the experimental observations. The mass origin of the fermions and gauge bosons is discussed in Section 1.3.6 below.

1.3.6 Higgs Mechanism

Massive gauge bosons in the Lagrangian 1.21 can be accommodated through the Brout-Englert-Higgs (BEH) mechanism, by introducing a complex scalar field ϕ in the spinor representation of $SU(2)_L$ doublet as [10],

$$\phi = \begin{pmatrix} \phi^+ \\ \phi^0 \end{pmatrix} \tag{1.30}$$

A new term in the SM Lagrangian $\mathcal{L}_{BEH}$ depending on this scalar field can be defined as,

$$\mathcal{L}_{BEH} = (D_\mu \phi)^\dagger (D^\mu \phi) - \mu^2 \phi^\dagger \phi + \lambda (\phi^\dagger \phi)^2 \tag{1.31}$$

The first term $(D_\mu \phi)^\dagger (D^\mu \phi)$ describes the kinematic of the new fields and the BEH potential $V(\phi)$ is given by the second term as,

$$V(\phi) = \lambda (\phi^\dagger \phi)^2 - \mu^2 \phi^\dagger \phi \tag{1.32}$$

The term $\lambda(\phi^\dagger \phi)^2$ describes the quartic self-interactions of the scalar fields and $\lambda > 0$ is imposed by the vacuum stability.

For $\mu^2 > 0$, the scalar field develops a nonzero Vacuum Expectation Value (VEV) which spontaneously breaks the symmetry. Due to the symmetry of $V(\phi)$ an infinite number of

degenerate states exists with the potential v only depending on the combination of $\phi^\dagger\phi$ [11] with minimum energy satisfying $\phi^\dagger\phi = \frac{v^2}{2}$. This minimum energy requirement reduces one of the four degrees of freedom of the complex scalar field ϕ. The three remaining degrees of freedom can be eliminated by a gauge transformation. We can choose ϕ by eliminating the upper component and the imaginary part of the lower component of the complex scalar field as,

$$< \phi >= \frac{1}{\sqrt{2}} \begin{pmatrix} 0 \\ v + H(x) \end{pmatrix}, \qquad ;, \; H(x) = H^*(x) \frac{1}{\sqrt{2}} \begin{pmatrix} 0 \\ v \end{pmatrix} \tag{1.33}$$

where the Higgs field (H) emerges as the excitation from the vacuum state. This choice of the minimum, spontaneously breaks the gauge symmetry [12].

After substituting the ϕ in the Lagrangian in equation 1.31, the kinetic term takes the form

$$\begin{aligned} \mathcal{L}_{BEH\ Kinetic} &= \tfrac{\lambda}{2} v^4 \\ &+ \tfrac{1}{2}\partial_\mu H \partial^\mu H - \lambda v^2 H^2 + \tfrac{\lambda}{\sqrt{2}} v H^3 + \tfrac{\lambda}{8} H^4 \\ &+ \tfrac{1}{4}(v + \tfrac{1}{\sqrt{2}} H)^2 (W^1_\mu \quad W^2_\mu \quad W^3_\mu \quad B_\mu) \begin{pmatrix} g^2 & 0 & 0 & 0 \\ 0 & g^2 & 0 & 0 \\ 0 & 0 & g^2 & gg' \\ 0 & 0 & gg' & g^2 \end{pmatrix} \begin{pmatrix} W^{1\mu} \\ W^{2\mu} \\ W^{3\mu} \\ B^\mu \end{pmatrix} \end{aligned} \tag{1.34}$$

where, the first line is the vacuum energy density and can be ignored in the case of QFT. The second line describes the triple and quartic self-interactions of the Higgs field as well as the mass term of the real scalar field H as $m_H = 2\lambda v^2$. The last line contains the mass term for the vector bosons.

From equations 1.34 and 1.24 is evident the mass of the two charged vector bosons $W^\pm$ is $m_W = \frac{1}{2} g^2 v^2$. Similarly, from equations 1.34 and 1.27, mass of the Z boson is

$m_Z = \frac{1}{2}(g^2 + g^{'})v^2$ and mass of the photon is $m_\gamma = 0$.

The initial $SU(2)_L$ Lagrangian in equation 1.31 started with four gauge symmetries, which is reduced to a single $U(1)_Q$ gauge symmetry associated with the massless vector field in equation 1.34. This phenomenon in the Higgs mechanism is called the Electroweak Symmetry Breaking (EWSB) mechanism. As discussed above, the EWSB mechanism is at the heart of the SM by which the gauge boson gets the mass which also arises the longitudinal polarization of the massive vector bosons. This thesis summarizes a measurement that has an experimental sensitivity to a such important property of the theory.

The last remaining piece in the SM is adding the fermion mass to the Lagrangian. A simple Lagrangian with the fermion mass can be written as,

$$\mathcal{L}_{mass\ fermion} = -m(\bar{\chi_L}\psi_R + \bar{\psi}_R\chi_L) \tag{1.35}$$

This term violates $SU(2)_L$ gauge symmetry because the left-handed fermions are doublets and the right-handed are singlets. Adding a scalar complex field $\phi = \frac{1}{\sqrt{2}}\begin{pmatrix} 0 \\ v + H(x) \end{pmatrix}$ in the Lagrangian becomes,

$$\mathcal{L}_{Yukawa,\ \ell} = \frac{G_\ell v}{\sqrt{2}}(\bar{\chi_L}\psi_R + \bar{\psi}_R\chi_L) - \frac{G_\ell}{\sqrt{2}}(\bar{\chi_L}\psi_R + \bar{\psi}_R\chi_L)H \tag{1.36}$$

with arbitrary parameters $G_{\ell=e,\mu,\tau}$. The constant in the first term $\frac{G_\ell v}{\sqrt{2}}$ represents the mass of the fermions, whereas the second term gives the interaction of fermions with the Higgs field.

Similarly, the mass terms for quarks follow but including the down-type quarks, the parameters corresponding to G_ℓ are matrices G_q^{ij} for the quark families i, j and up-type and down-type quarks as:

$$\mathcal{L}_{Yukawa,\ Q} = -G_d^{ij}(\bar{u}_i, \bar{d}_i)_L\phi d_{jR} - G_u^{ij}(\bar{u}_i, \bar{d}_i)_L\phi u_{jR} + h.c. \tag{1.37}$$

The final Standard Model Lagrangian is the sum of the QED (equation 1.9), QCD (equation 1.16), Boson self-interactions (equation 1.21), Higgs potential and self-interactions (equation 1.31), and the Higgs-fermion Yukawa coupling (equations 1.36 & 1.37), which in a compact form is written in equation 1.1.

2 Limitations of the Standard Model

The predictions of the Standard Model have been experimentally validated by many discoveries since the 20^{th} century. The breakthrough discovery of the Higgs boson in 2012 at the LHC validated the last piece of the theory [13]& [14]. Many predicted parameters such as production cross-sections and decay branching ratios for several processes have been measured with high precision. No statistically significant discrepancy from theory has been observed except for the $W^{\pm}$ boson mass measurement from the CDF II Collaboration [15].

Despite the incredible success of the theory, experimental evidence suggests that the theory is incomplete. SM has the following limitations:

- SM fails to explain the gravitational force.
- SM only describes 5% of the universe. It fails to explain dark matter whose existence is experimentally supported by astrophysical observations such as galactic rotation curves and gravitational lensing [16]. It also doesn't explain dark energy.
- The CP violation allowed in SM cannot explain the amount of anti-matter asymmetry observed in the universe.
- The strengths of the four fundamental forces are different by many orders of magnitude. It is not yet understood the hierarchy of such interactions.

These limitations suggest that the SM is an effective field theory, only describing an approximation of our universe. Thus, motivating the experimental searches for new physics beyond the Standard Model (BSM).

3 Phenomenology of Proton-Proton Collisions

The main results discussed in this thesis are differential cross-sections for di-Z boson production in association with two jets in a proton-proton collider at the center of mass energy of $\sqrt{s} = 13\ TeV$. Protons are composite particles made up of quarks and gluons. Thus the theoretical formalism discussed above doesn't provide all the necessary tools for experimental cross-section measurements in hadron colliders. The differential cross-section $d\sigma$ for two particles is given by,

$$d\sigma = \frac{|\mathcal{M}|^2}{F} dQ \tag{3.1}$$

where F is the incident flux and dQ represents the Lorentz invariant phase space factor. The scattering amplitude $\mathcal{M}$ is the matrix element calculated from the Lagrangian density of the SM using a perturbative expansion [17].

The cross-section of a process with two initial-state partons p_1 and p_2 producing the final state X is given by:

$$d\sigma_{p_1 p_2 \to X} = \int dx_1 dx_2 \sum_{q_1, q_2} f_{q_1}(x_1, \mu_F) f_{q_2}(x_2, \mu_F) d\sigma_{q_1 q_2 \to X}(x_1, x_2, \mu_F, \mu_R) \tag{3.2}$$

where, q_1, q_2 are the partons of the protons, and $d\sigma_{q_1 q_2 \to X}(x_1, x_2, \mu_F, \mu_R)$ is the partonic cross-section. The functions $f_{q_1}(x_1, \mu_F)$ & $f_{q_2}(x_2, \mu_F)$ are the parton distribution functions (PDF) representing the density of the partons q inside a proton carrying the longitudinal momentum fraction x. The PDFs are determined experimentally using data from deep-inelastic-scattering, jets production, and Drell Yan events [18] [19]. As shown by figure 2, a PDF of a parton depends on the reference value of the momentum transfer Q_0^2. The differences are driven by modifications of the partons' momenta resulting from the emission of gluons off of quarks and the splitting of gluons to $q\bar{q}$ pairs. A PDF at any value of Q^2 can be calculated using the PDF at reference scale Q_0^2. The factorization scale μ_F determines

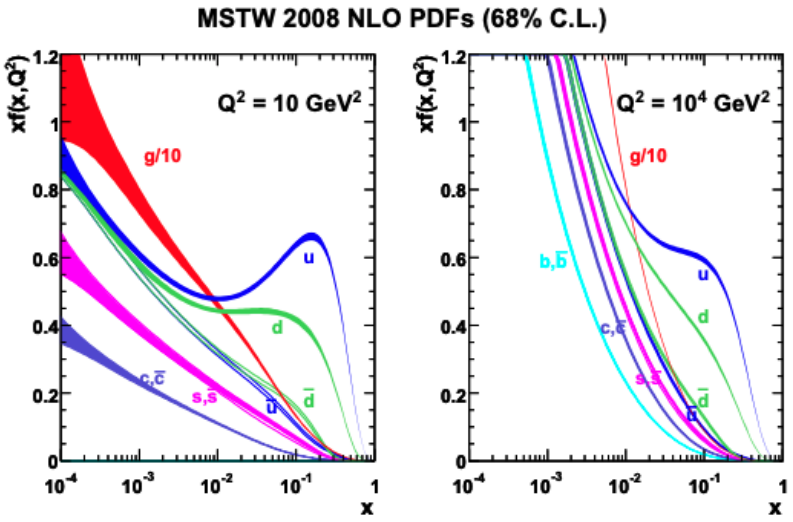

Figure 2: Parton distribution functions $xf_q(x, Q^2)$ for reference momentum transfer $Q_0^2 = 10\ GeV^2$ (left) and $Q_0^2 = 10^4\ GeV^2$ (right). The dependence of momentum fraction z carried by a parton is extracted in global PDF fits from experimental data [4].

the threshold whether the perturbative corrections modify the PDF or are included in the partonic cross-sections $d\sigma_{q_1 q_2}$ [17].

The partonic cross-section is calculated perturbatively as an expansion in terms of the strong coupling constant α_S as,

$$d\sigma_{q_1 q_2 \to X} = \alpha_S^k \sum_{m=0}^{n} c_m \alpha_S^m \tag{3.3}$$

The coefficient c_m depends on the center-of-mass energy s and theoretical calculations usually contain a finite number of coefficients. Leading order (LO) calculations include one term ($n = 0$), whereas next-to-leading order (NLO) and next-to-next-to-leading order (NNLO) contains two ($n = 1$) and three ($n = 2$) terms respectively. The theoretical calculations relevant to the thesis are generally calculated at NLO. The higher-order terms in the series contain additional virtual loop contributions and real emissions of quarks and gluons. The presence of virtual loops beyond the LO introduces singularities in the calculation of scattering amplitudes. The divergences are controlled via the renormalization procedure, where the

singularities are absorbed by reparametrization of the coupling and mass parameters. The renormalization process is energy-dependent. Therefore, the predicted cross-sections from theoretical calculations are dependent on the renormalization scale μ_R and factorization scale μ_F. The scale dependence is varied in Monte Carlo simulations to derive uncertainties on the predicted cross-section due to missing higher-order contributions.

The additional partons of the two protons that interact in the hard interaction process lead to minor energy deposits in the detector referred to as an underlying event. Any outgoing partons from the interaction emit multiple QCD radiation via the parton showering process, where the energy of each parton is split among an increasing number of other elementary particles. Due to the color confinement nature of QCD, at lower energies of the order of the pole of the QCD running coupling (λ_{QCD}), the partons are bound into stable and unstable hadrons. This process is named as hadronization and leads to the formation of collimated sprays of charged and neutral hadrons in the detector called jets. Figure 3, shows schematically the phenomenology of di-Z boson production in association with two jets in the proton-proton collider. The theoretical predictions of such events are calculated using Monte Carlo (MC) simulations which include matrix element calculations for two partons giving two Z bosons, the parton showering, the effect of the underlying events, hadronizations, and pile-up. A comprehensive overview of the methods used in MC simulation is discussed in Ref [20].

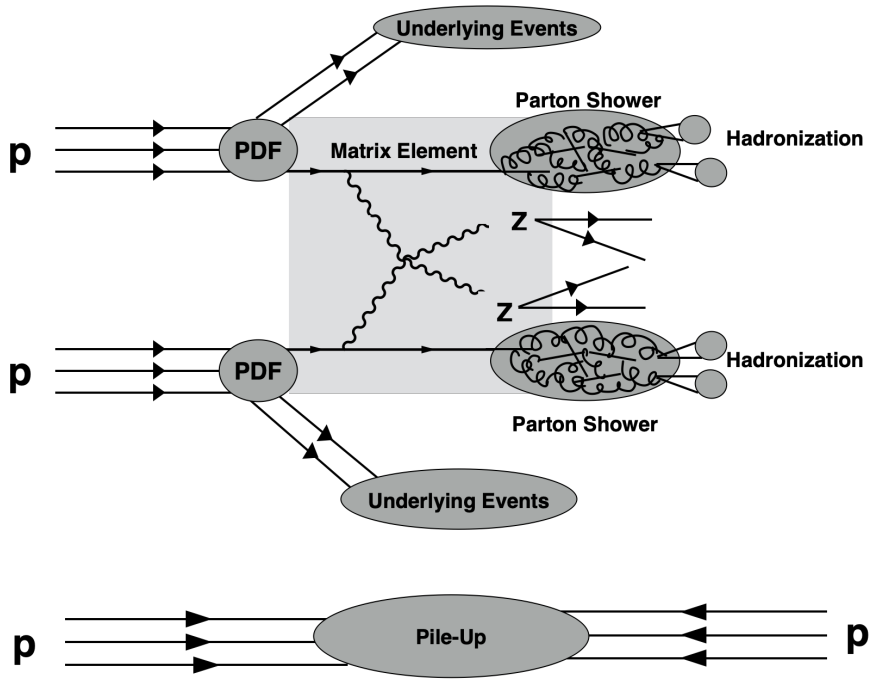

Figure 3: Phenomenology of di-Z boson production in association with two jets in proton-proton collider

4 Electroweak Diboson Physics

In LHC, two types of physics processes, the QCD production at the order $\alpha_S^2\alpha_{EWK}^4$ and the EWK production at order α_{EWK}^6 contribute to the production of di-Z bosons in an association of two jets ($ZZjj$) [21]. Figure 4 shows the Feynman diagram at leading order for the QCD ZZjj process, whereas figure 5 shows the Feynman diagram at leading order for the EWK production of ZZjj [22]. The EWK production consists of two sets of interactions, first, the Vector Boson Scattering processes involving either triple (figure 5a) or quartic (figure 5b) self-interactions of the gauge-bosons, and second the diagrams featuring the Higgs bosons (figure 5c & 5d). The scattering amplitudes of the VBS processes involving longitudinally polarized vector bosons, grow quadratically with the center of mass energy ($\sqrt{s}$), eventually violating the unitarity bounds. The precise SM interference between the Higgs-featured process and the VBS process restores the unitarity [23]. As discussed in Section 1.3.6, the massive W and Z bosons get their masses via the BEH mechanism through EWSB. As a consequence of EWSB, the W and Z bosons acquire an additional degree of freedom (the longitudinal polarization mode) whose scattering interfere with the Higgs featured processes. Thus, the study of electroweak production of the di-Z bosons in association with two jets provides a direct probe of the EWSB, which is at the heart of the SM [21].

The triple and quartic self-interactions of the gauge bosons arise from the non-Abelian structure of $SU(2)$ in the kinetic term $\frac{1}{4}W^a_{\mu\nu}W^{\mu\nu}_a$ of the EWK Lagrangian in equation 1.21. Implementing the values of the field strength tensor $W^a_{\mu\nu}$ from equation 1.23, the relations of $W^{\pm}_{\mu}$ fields in equation 1.24, and the relations of neutral gauge fields in equation 1.27, the triple and quartic self interaction terms become,

$$\mathcal{L}_3 = ie_{V=\gamma,Z}[W^+_{\mu\nu}W^{-\mu}V^{\nu} - W^-_{\mu\nu}W^{+\mu}V^{\nu} + W^+_{\mu}W^-_{\nu}V^{\mu\nu}] \tag{4.1}$$

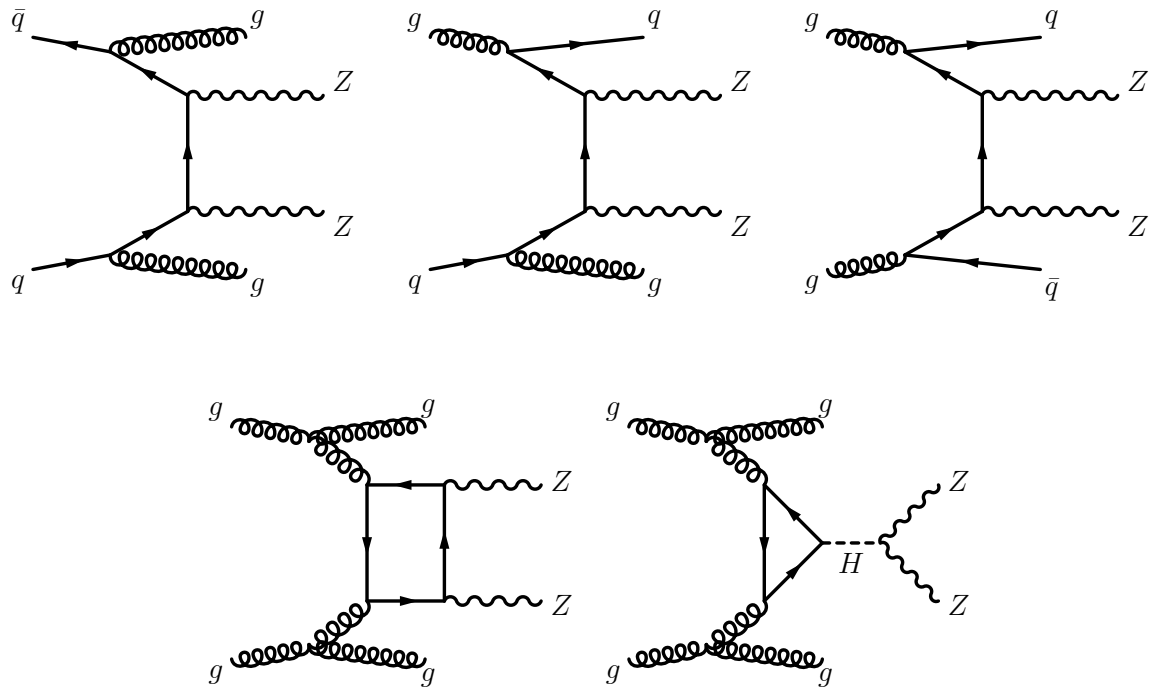

Figure 4: Typical diagrams for the QCD $\alpha_S^2\alpha_{EWK}^4$ production of $ZZjj$.

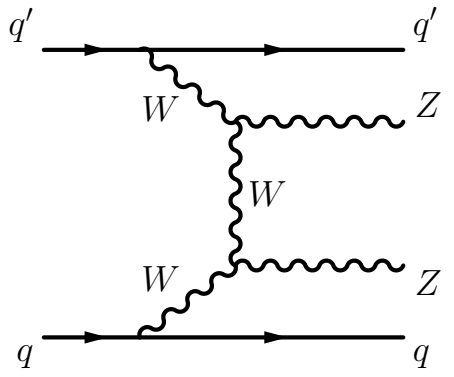

(a) ZZjj production with two triple gauge coupling (TGC) vertices.

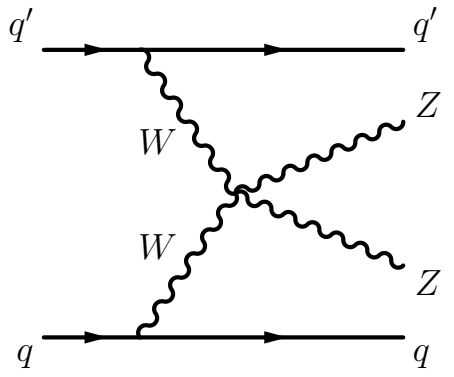

(b) ZZjj production with a quartic gauge coupling (QGC) vertex.

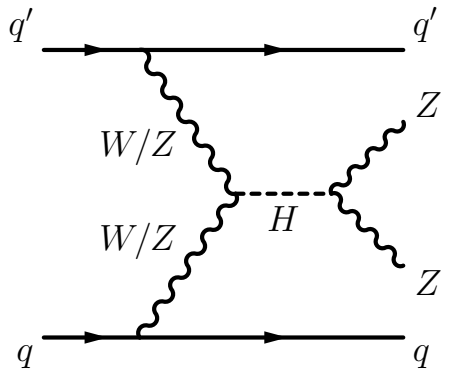

(c) s-channel Higgs ZZjj Production.

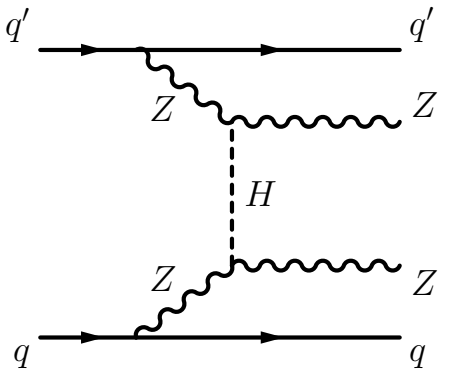

(d) t-channel Higgs ZZjj Production.

Figure 5: Feynman diagrams at LO for the EWK α^6_{EWK} production of $ZZjj$.

$$\begin{aligned}\mathcal{L}_4 &= e_W^2[W_\mu^- W^{+\mu} W_\nu^- W^{+\nu} - W_\mu^- W^{-\mu} W_\nu^+ W^{+\nu}] \\ &+e_{V=\gamma,Z}^2[W_\mu^- W^{+\mu} V_\nu V^\nu - W_\mu^- V^\mu W_\nu^+ Z^\nu] \\ &+e_\gamma e_Z[2W_\mu^- W^{+\mu} Z_\nu A^\nu - W_\mu^- Z^\mu W_\nu^+ A^\nu - W_\mu^- A^\mu W_\nu^+ Z^\nu]\end{aligned} \tag{4.2}$$

where, $e_\gamma = gsin\theta_W$; $e_W = \frac{e_\gamma}{2\sqrt{2}sin\theta_W}$ & $e_Z = e_\gamma cot\theta_W$ are the precise coupling strengths for vector boson self-interaction. Both triple and quartic neutral couplings such as ZZZ or $ZZZZ$ are absent in the SM.

Similarly, the couplings of Higgs to vector bosons are also predicted precisely by the BEH

mechanism in equation 1.34 as:

$$\mathcal{L}_{HVV} = \frac{m_W^2}{v^2} W_\mu^+ W^{-\mu} h^2 + \frac{m_Z^2}{v^2} Z_\mu Z^\mu h^2 \tag{4.3}$$

The EWK production of $ZZjj$ is extremely sensitive to any possible anomalous triple gauge couplings (aTGC), anomalous quartic gauge couplings (aQGC), or anomalous Higgs to vector boson coupling [24] [25] [26] . Therefore, it is imperative to probe the high energy behavior of the EWK production of $ZZjj$ to seek possible deviations arising from the physics processes beyond the Standard Model (BSM).

The EWK $ZZjj$ production with each Z boson decaying to a pair of same-flavor opposite-sign (SFOS) lepton pairs is an extremely rare process. Moreover, with limited statistics in Run-2 the QCD background processes dominate the $ZZjj \to 4\ell jj$ final state [27]. Therefore, the differential cross-sections discussed in this thesis are measured in a VBS-enhanced phase space with a high fraction of events resulting from the EWK $ZZjj$ process. The enhanced phase space relies on the characteristic feature of the EWK process with two jets (jj) in the forward-backward region originating from the scattered quarks. These jets have large rapidity separation with no additional hadronic activity from the hard scattering between the two jets [28]. The decay of the two Z bosons into SFOS muons or electron pairs defines the final signature of the VBS-$ZZjj$-like event.

Chapter III: The Large Hadron Collider

5 ATLAS Detector

6 Particle Reconstruction

7 Future Upgrades

Chapter IV: Analysis Overview

This section discussed the overview of the analysis

8 Goals

9 Datasets and Monte Carlo Simulation

10 Phase Space Definition

11 Object and Event Selection

12 Definition of Measured Observables

Chapter V: Analysis Strategy

13 Background Estimation

14 Unfolding

15 Uncertainties on the Measurement

Chapter VI: Results

16 Differential Cross-sections

17 Effective Field Theory ReInterpretation

Chapter VII: Conclusion

Chapter VIII: Outlook

18 Run-3

19 High Luminosity LHC

References

[1] P.A. Zyla et al. Review of Particle Physics. *PTEP*, 2020(8):083C01, 2020.

[2] Francis Halzen and Alan Martin. *Quarks & Leptons: An introductory course in modern particle physics*. John Wiley & Sons, New York, USA, 1984.

[3] Wikipedia contributors. Standard Model of Elementary Particles. https://en.wikipedia.org/wiki/Standard_Model, 2019. [Online; accessed 05-November-2022].

[4] A. D. Martin, W. J. Stirling, R. S. Thorne, and G. Watt. Parton distributions for the LHC. *Eur. Phys. J. C*, 63:189–285, 2009.

[5] Mark Thomson. *Modern particle physics*. Cambridge University Press, New York, 2013.

[6] E. Noether. Invariante variationsprobleme. *Nachrichten von der Gesellschaft der Wissenschaften zu Göttingen, Mathematisch-Physikalische Klasse*, 1918:235–257, 1918.

[7] Bernabeu, Jose", and Murillo, Jesús Carnicer and Michelini, Marisa and Perea, Carmen. *Fundamental Physics and Physics Education Research*, chapter Symmetries in the Standard Model, pages 3–16. Springer International Publishing, Cham, 2021.

[8] Sheldon L. Glashow. Partial-symmetries of weak interactions. *Nuclear Physics*, 22(4):579–588, 1961.

[9] C. N. Yang and R. L. Mills. Conservation of Isotopic Spin and Isotopic Gauge Invariance. *Phys. Rev.*, 96:191–195, Oct 1954.

[10] Nguyen, K. The Higgs Mechanism, 2009.

[11] M. E. Peskin , D. V. Schroeder. *An Introduction to Quantum Field Theory*. Westview PRESS, Colorado, USA, 1995.

[12] Buchmüller, W. and Lüdeling, C. Field Theory and Standard Model, 2006.

[13] CMS Collaboration. Observation of a new boson at a mass of 125 GeV with the CMS experiment at the LHC. *Physics Letters B*, 716(1):30–61, sep 2012.

[14] The ATLAS Collaboration. Observation of a new particle in the search for the Standard Model Higgs boson with the ATLAS detector at the LHC. *Physics Letters B*, 716(1):1–29, 2012.

[15] The CDF II Collaboration. High-precision measurement of the W boson mass with the CDF II detector. *Science*, 376(6589):170–176, 2022.

[16] Richard Massey, Thomas Kitching, and Johan Richard. The dark matter of gravitational lensing. *Reports on Progress in Physics*, 73(8):086901, jul 2010.

[17] Peter Skands. QCD for Collider Physics, 2011.

[18] Sergey Alekhin, Kirill Melnikov, and Frank Petriello. Fixed target Drell-Yan data and NNLO QCD fits of parton distribution functions. *Phys. Rev. D*, 74:054033, Sep 2006.

[19] Sergey et al. Alekhin. The PDF4LHC Working Group Interim Report, 2011.

[20] Andy Buckley et al. General-purpose event generators for LHC physics. *Physics Reports*, 504(5):145–233, 2011.

[21] The CMS Collaboration. Evidence for electroweak production of four charged leptons and two jets in proton-proton collisions at s=13TeV. *Physics Letters B*, 812:135992, 2021.

[22] Jager, B., Karlberg, A. and Zanderighi, G. . Electroweak ZZjj production in the Standard Model and beyond in the POWHEG-BOX V2. *J. High Energ. Phys.*, 141, 2014.

[23] A. Denner and T. Hahn. Radiative corrections to W+W- → W+W- in the electroweak standard model. *Nuclear Physics B*, 525(1-2):27–50, 1998.

[24] Tao Han and David Krohn and Lian-Tao Wang and Wenhan Zhu. New physics signals in longitudinal gauge boson scattering at the LHC. *J. High Energ. Phys.*, 2010(3), mar 2010.

[25] Eduardo da Silva Almeida and O. J. P. Éboli and M. C. Gonzalez–Garcia. Unitarity constraints on anomalous quartic couplings. *Physical Review D*, 101(11), jun 2020.

[26] Jung Chang, Kingman Cheung, Chih-Ting Lu, and Tzu-Chiang Yuan. WW Scattering in the Era of Post Higgs Discovery. *Physical Review D*, 87(9), may 2013.

[27] ATLAS Collaboration. Observation of electroweak production of two jets and a Z-boson pair, 2020.

[28] Khoze, V., Ryskin, M., Stirling, W. et al. A Z-monitor to calibrate Higgs production via vector boson fusion with rapidity gaps at the LHC. *Eur. Phys. J.*, C 26:429–440, 2003.

Appendices